RESEARCH PAPER

Effect of Pulse Electrodeposition Parameters on the Properties of Ni-Co/SiC-CeO₂ Composite Coatings on Copper Substrates

Mehdi Mehranian, Hajar Ahmadimoghadam*

* hajar.ahmadi@sku.ac.ir

Materials Engineering Department, Faculty of Engineering, Shahrekord University, Shahrekord, Iran

Abstract: *In this research study, a composite coating of Ni-Co/SiC-CeO₂ was prepared on a copper substrate using the pulse electrodeposition technique. The effects of electrodeposition parameters, including current density, duty cycle, and frequency, on the properties of the prepared coating were investigated. The selected current density values were 0.1, 0.2, and 0.3 A/cm², the duty cycle options were 10, 20, and 30%, and the frequency values were 10, 100, and 1000 Hz. Increasing the current density enhanced the microhardness of the coating but reduced its corrosion resistance. This behavior can be attributed to the grain refinement occurring within the coating as the current density increases. On the other hand, an increase in the duty cycle resulted in a decrease in microhardness, which can be attributed to a decrease in the concentration of nanoparticles within the coating. The lower corrosion resistance observed at higher duty cycles could be attributed to the decrease in off-time, causing the pulse electrodeposition conditions to approach a DC (direct current) state. Furthermore, higher frequencies were found to be associated with increased microhardness and improved corrosion resistance of the coatings. The coatings with the highest corrosion resistance exhibited a corrosion current density of 0.29 μA/cm² and a polarization resistance of 1063 Ω.cm² in a 3.5% NaCl solution. These coatings were prepared using a current density of 0.2 A/cm², a duty cycle of 10%, and a frequency of 1000 Hz.*

Keywords: *Ni-Co/SiC-CeO₂ coatings, Current density, Duty cycle, Frequency, Corrosion resistance.*

1. INTRODUCTION

Composite coatings have received significant attention in both scientific and industrial circles due to their exceptional properties, which include excellent wear resistance, high corrosion resistance, and a high level of hardness [1, 2]. These coatings can be manufactured using various techniques, such as physical vapor deposition (PVD), chemical vapor deposition (CVD), ion implantation, and electrodeposition. Among these methods, electrodeposition stands out due to its numerous advantages. It offers a cost-effective solution with the potential for scalability in industrial applications, ease of implementation, versatility in terms of composition, size, and shape, as well as a high production rate. Given these advantageous attributes, electrodeposition is the preferred method for the fabrication of composite coatings [2-4].

Electrodeposition is a promising technique for the fabrication of metal matrix composites incorporating micro or nano-sized ceramic particles. Previous studies have shown that compared to direct current (DC) electrodeposition, pulse current (PC) electrodeposition can produce coatings with enhanced characteristics in terms of morphology, particle distribution, structure, grain size, hardness, and wear resistance [5-7]. PC electrodeposition has been successfully used to prepare nickel matrix composites with various ceramic particles, such as SiC, P-SiC, Al_2O_3, and TiO_2 [2, 6, 8]. In PC electrodeposition, three crucial parameters significantly affect the properties of the coating: the duration of pulse application (known as pulse on-time, t_{ON}), relaxation time (off-time, t_{OFF}), and peak current (IP). The relationships among these parameters can be expressed as follows, where d represents the duty cycle and f denotes the frequency [7, 8].

$$d= t_{ON}/(t_{ON}+t_{OFF})= t_{ON}\, f \qquad (1)$$
$$f= 1/(t_{ON}+t_{OFF}) \qquad (2)$$

The special properties of Ni-Co alloys, such as strength, corrosion resistance, wear resistance, electrocatalytic properties, and magnetic characteristics, have garnered significant attention in various industries, including magnetic storage, automotive, electrical, and aerospace sectors [7-10]. However, there is an ongoing need to improve their corrosion and wear resistances to extend their lifespan and broaden their applicability in harsh environments, such as marine engineering, mining, oil, and chemical industries [10, 11]. Recent research efforts have focused on enhancing Ni-Co composite coatings by incorporating nanoparticles to optimize

Hajar Ahmadimoghadam et al.

their performance and meet specific practical requirements. Researchers have investigated the incorporation of different ceramic particles, such as SiO_2, Al_2O_3, SiC, Cr_2O_3, TiO_2, ZrO_2, and others, into nickel-cobalt electrolytes to assess their impact on the mechanical properties and corrosion behavior of Ni-Co coatings [2, 6, 10-12]. The research results show that the addition of SiC nanoparticles greatly influenced the hardness and corrosion resistance of Ni-Co coatings [8, 13-16]. The incorporation of CeO_2 nanoparticles in Ni-Co coatings resulted in enhanced microhardness, wear resistance and thermal stability. The improved corrosion resistance of $Ni-Co/CeO_2$ composite coatings could be attributed to a considerable reduction in porosity [17-20].

It is crucial to control the parameters of pulse electroplating to obtain coatings with desirable properties and characteristics. Parameters such as current density, duty cycle, and frequency of pulse electroplating have significant impacts on the properties of the coatings, including surface morphology, grain size, grain orientation, the quantity of deposited nanoparticles in the coating, microhardness, and corrosion resistance [7]. Yang et al. [8] investigated the impact of duty cycle and frequency on the characteristics of Ni-Co/SiC coatings. Their findings revealed that reducing the duty cycle led to increased microhardness and corrosion resistance. This was attributed to a higher concentration of SiC nanoparticles in the coating. Yu et al. [15] demonstrated that Ni-Co/SiC coatings, prepared at a frequency of 10 Hz and a duty cycle of 10%, exhibited higher microhardness due to a greater presence of SiC. Additionally, they found that the coatings displayed improved corrosion resistance with increasing frequency [15]. Increasing the current density in Ni-Co/SiC coatings resulted in a decrease in cobalt content and a structural transformation from face-centered cubic (FCC) to hexagonal close-packed (HCP) [21]. It was reported that with increasing current density, the cathode experienced enhanced hydrogen evolution reaction, the surface roughness increased, nanoparticles further agglomerated, and the grains of the Ni-Co coating became more refined [7].

Based on the reported findings, the incorporation of CeO_2 and SiC nanoparticles has the potential to improve the performance of Ni-Co coatings. This study introduces a novel approach by using SiC and CeO_2 nanoparticles together as reinforcement materials in Ni-Co coatings. The main objective is to investigate the electrodeposition parameters associated with this methodology. Therefore, the effects of current density, duty cycle, and frequency on various properties of the Ni-Co/SiC-CeO_2 coatings, including microhardness and corrosion resistance, were investigated.

2. EXPERIMENTAL PROCEDURES

Copper sheets with a purity of 99% and dimensions of 0.5 cm × 2 cm × 5 cm were used as the substrate (cathode). The anode material consisted of a nickel sheet with a purity of 99.9% and dimensions of 0.5 cm × 2 cm × 5 cm. To achieve a mirror-like surface on the substrate, the copper sheets were initially polished using polishing paper ranging from 500 to 2500 grit, followed by a felt cloth. The cathode was degreased and cleansed of impurities by immersing it in a solution of acetone and ethanol for 15 minutes, followed by rinsing with distilled water. To activate the cathode surface, a 1:1 HCl solution was used for 30 s, followed by another rinse with distilled water. The cathode had a surface area of 4 cm^2 that came into contact with the electrolyte.

Table 1 shows the chemical composition of the electrolyte and electrodeposition parameters. The materials used in this study are sourced from the Mark Company and have a purity greater than 99%.

Table 1. Electrolyte composition and electrodeposition parameters Ni-Co–SiC-CeO_2 coatings

Electrolyte formula (g/l)		Process parameters	
$NiSO_4.6H_2O$	200	Temperature	45-50°C
$NiCl_2.6H_2O$	10	pH	4-4.5
$CoSO_4.6H_2O$	25	Current mode	pulse current
H_2BO_3	25	Current density	0.1, 0.2, 0.3 A/cm^2
SiC nanoparticles	5	Duty cycle (d)	10, 20, 30%
CeO_2 nanoparticles	5	Frequency (f)	10, 100, 1000 Hz
Sodium dodecyl sulfate (SDS)	0.1		

2

The pH of the bath was adjusted utilizing ammonia or hydrochloric acid. Furthermore, silicon carbide (SiC) and cerium oxide (CeO₂) nanoparticles with an approximate size of 15 to 30 nm and a purity of 99% were used to reinforce the Ni-Co coatings. To prevent the agglomeration of SiC and CeO₂ nanoparticles, a surfactant called sodium dodecyl sulfate (SDS) was included in the bath. The sources of Ni and Co were nickel sulfate and cobalt sulfate, respectively. Nickel chloride was used to facilitate the dissolution of the anode.

Before starting the electrodeposition process, the electrolyte bath was stirred for 24 hours using a magnetic stirrer at a speed of 1000 rpm. After that, it underwent a 30-minute treatment in an ultrasonic bath and a subsequent 15-minute treatment using an ultrasonic probe. A Silicon Tuan International Company model SL120-PRC pulsed power supply was used to facilitate the electrodeposition of the samples with pulsed current. This device is capable of generating both square and reverse square waves, with a frequency range of 0.1 to 10 kHz. The deposition conditions for the Ni-Co-SiC-CeO₂ composite coatings are presented in Table 1. Fig. 1 illustrates the process involved in the production method of the coating mentioned above.

The Field Emission Scanning Electron Microscope (FESEM, Sigma VP, ZEISS) was used to investigate the surface morphology and analyze the coatings. The FESEM was equipped with an X-ray Energy Dispersive Spectrometer (EDS).

To identify the phases in the coatings, a PANalytical (XPert Pro) X-ray Diffraction (XRD) machine was used. The XRD machine operated at a voltage of 60 kV with Cu Kα radiation (λ= 1.5418 Å) and a step size (2θ) of 0.05°. The microhardness of the coatings was measured using the Bowers model microhardness device. An applied load of 15 grams was used for 10 seconds. Each sample was tested five times, and the average values were reported. For the corrosion behavior analysis, a 3.5% NaCl solution was used in a three-electrode electrochemical cell with a capacity of 500 ml for the Tafel polarization test. The polarization curves of the coatings were obtained using the Auto Lab PG ST 302 N device. The scanning rate was set at 1 mV/s within the ±500 mV range. The substrates were immersed in the solution for 60 minutes at open-circuit potential (OCP) to stabilize the contact surface between the substrate and the solution. The obtained results were analyzed using Nova 1.8 software. The Tafel extrapolation method was employed to determine the corrosion current, corrosion voltage, and polarization resistance. The Stern–Geary equation establishes a relationship between polarization resistance and the corrosion current (i_{corr}), as presented below:

$$R_p = B/i_{corr} \tag{3}$$

The constant B acts as the proportionality factor, determined by the anodic (b_a) and cathodic (b_c) Tafel slopes, as explained below [21]:

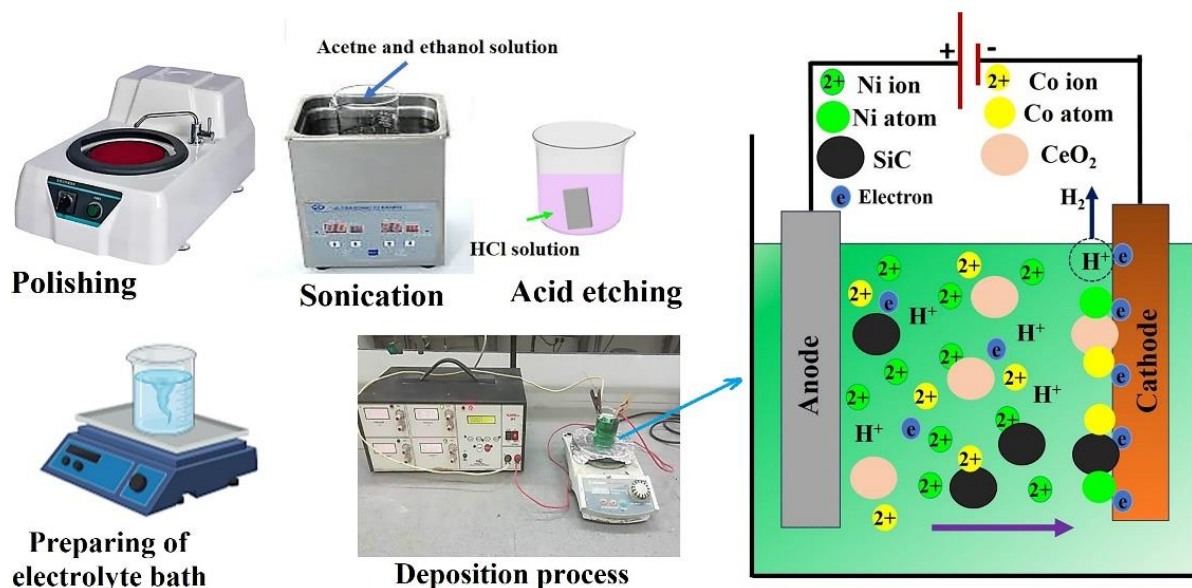$$B = b_a b_c/(2.303 i_{corr}(b_a+b_c)) \tag{4}$$

Fig. 1. Schematic diagram of the pretreatment and deposition process of coatings

3. RESULTS AND DISCUSSION

3.1. Investigating the Effect of Current Density

To investigate the effect of current density, coatings were prepared using current density values of 0.1, 0.2, and 0.3 A/cm². These coatings were prepared at a frequency of 10 Hz and a duty cycle of 10 %. Fig. 2 illustrates the XRD patterns of the prepared coatings at different current densities. The identified peaks in the patterns correspond to nickel, exhibiting a face-centered cubic (FCC) structure. The standard card number for nickel is PDF No. 3025-901-96. Three peaks at angles of approximately 44.3°, 51.6°, and 76.3° correspond to the (111), (200), and (220) planes, respectively. Both Co and Ni possess an FCC cubic lattice, with closely matched atomic radii. Consequently, it is feasible to position cobalt atoms within the Ni lattice. These XRD patterns illustrate that the coatings' matrix is composed of a solid solution of Co in Ni [10, 12]. The absence of prominent peaks of SiC and CeO_2 is due to their low volume percentage in the coatings [12]. From Fig. 2, it is evident that the intensity of peaks related to the (111) planes increases with the increase in current density. Previous studies have reported that as the current density increases, favorable conditions for the deposition of Ni metal ions arise. Consequently, the amount of Ni in the coating increases, while the quantity of cobalt and oxide particles decreases. As a result of this increase in current density, growth is observed to increase in the (111) planes and decrease in the (200) and (220) planes [7, 21]. At higher current densities, the intensity of the (200) peaks diminishes due to several interrelated factors. Firstly, an increase in current density often results in smaller grain sizes, which is attributed to rapid nucleation and limited growth time. This phenomenon leads to broader diffraction peaks and reduced intensity. Additionally, changes in preferred orientation may occur; if the (200) orientation is less favored, its peak intensity decreases relative to other orientations. Furthermore, alterations in deposition kinetics impact microstructure and crystallinity, while an increase in defect density, such as dislocations and vacancies, enhances X-ray scattering. Collectively, these effects significantly influence the structural properties of the coatings [7, 12, 21].
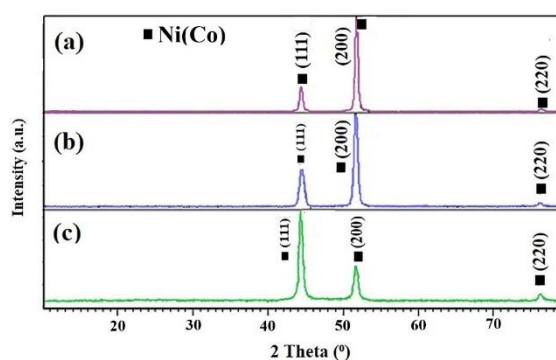
Fig. 2. XRD pattern of the coatings obtained at a frequency of 10 Hz, duty cycle of 10%, and current density of a) 0.1, b) 0.2, and c) 0.3 A/cm²

Fig. 3 illustrates the morphological characteristics of the coatings at different current densities. It is evident from Fig. 3 that the microstructure of the coatings becomes finer as the current density increases. Based on Fig. 3, the average grain sizes of the coatings prepared at current densities of 0.1, 0.2, and 0.3 A/cm² are approximately 48 nm, 35 nm, and 15 nm, respectively. This change in microstructure can be attributed to the higher discharge rate of ions at higher current densities. As a result, more new nuclei are formed, leading to smaller grain sizes [7, 10]. Moreover, it has been reported that increasing the current density reduces the roughness of the coating surface. This reduction in roughness indicates a shift in the growth mechanism from a planar state to the formation of spherical and columnar fine grains [10, 21] Increasing current density improves surface refinement by enhancing mass transport and electrochemical kinetics. At higher densities, diffusion, and ion movement toward the electrode surface increase, which reduces concentration gradients and enables uniform deposition. Convection currents in the electrolyte also help by supplying reactants and removing byproducts. Faster reaction rates promote consistent material deposition and smoother nucleation, minimizing surface roughness. Additionally, higher current densities encourage smaller grain formation and reduce surface irregularities, resulting in a smoother surface through optimized deposition and fewer defects [7, 10, 21].

Fig. 4 presents the results of Energy Dispersive Spectroscopy (EDS) analysis for the coatings prepared at different current densities. The EDS analysis shows that an increase in the current density leads to a decrease in the amount of cobalt and nanoparticles present in the coating.
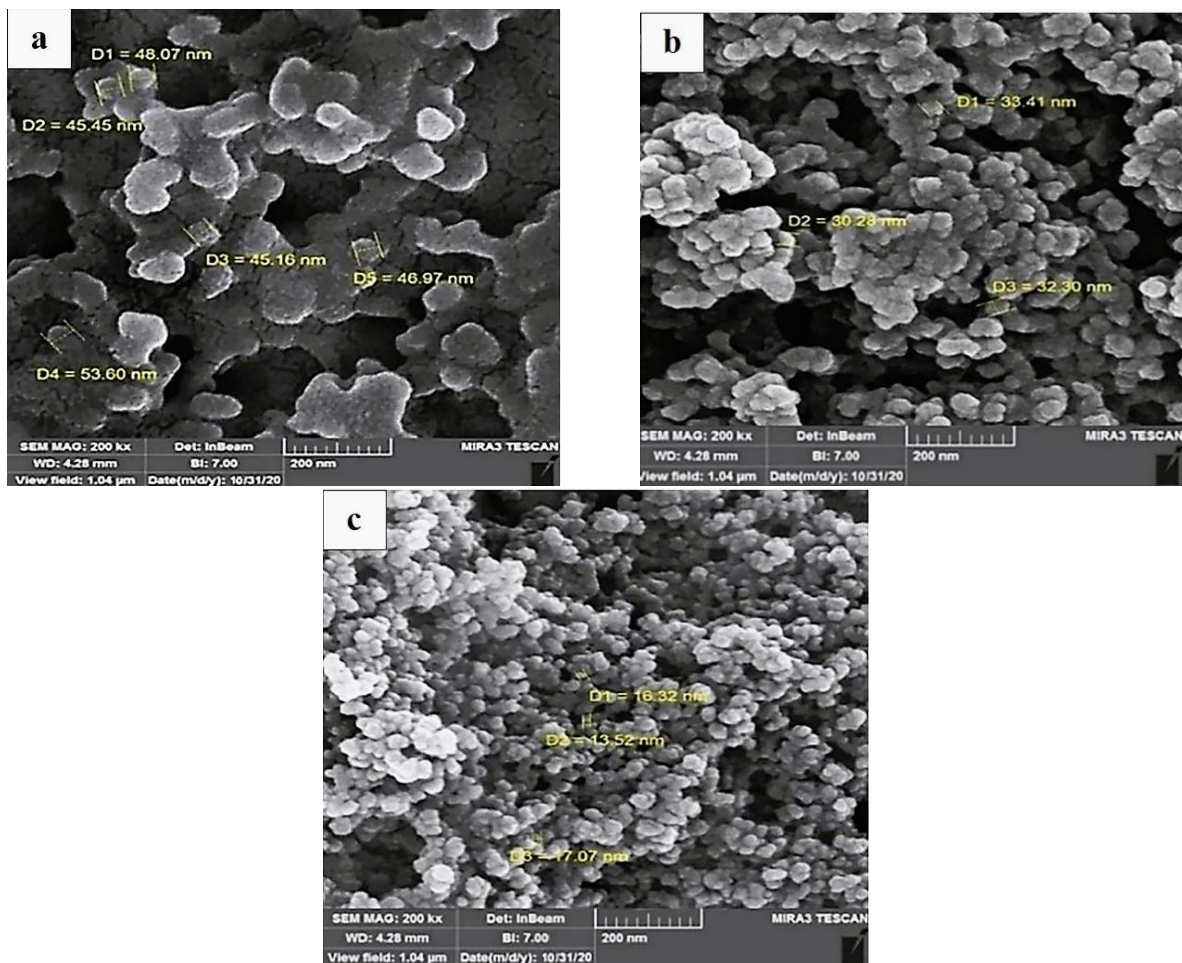
4

Fig. 3. SEM images of the coatings obtained at a frequency of 10 Hz, duty cycle of 10%, and current density of a) 0.1, b) 0.2, and c) 0.3 A/cm^2
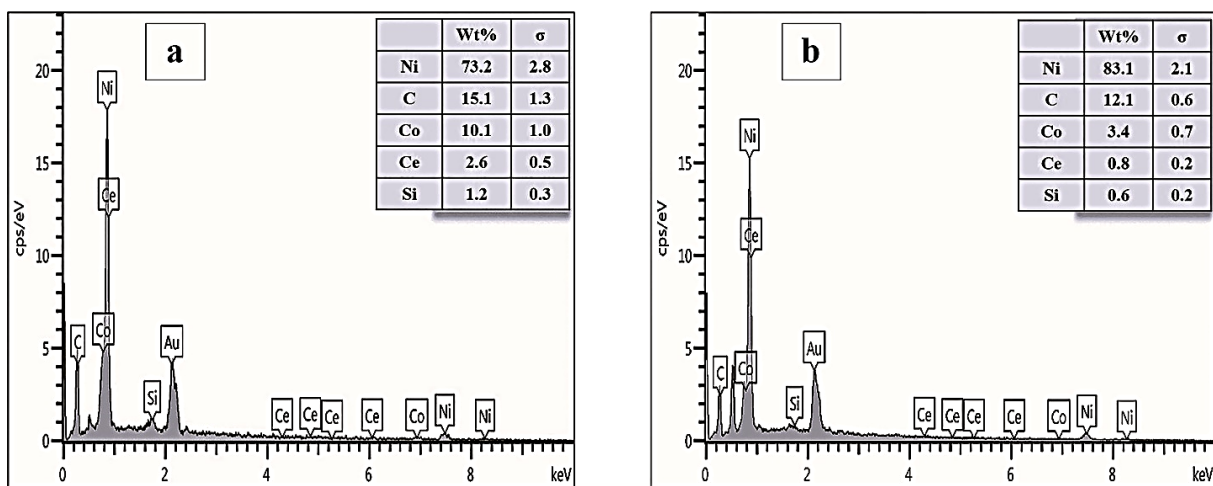

Fig. 4. EDS results of the coatings obtained at a frequency of 10 Hz, duty cycle of 10%, and different current densities: a) 0.1, and b) 0.3 A/cm^2

The weight percentage of cobalt and nanoparticles in the coating decreases as the current density increases. During the electrochemical process, free ions and ions on the surface of particles are attracted to the cathode. Free ions have higher mobility than ions on the particle surface, so a higher current density results in faster absorption of free ions by the cathode. This,

5

in turn, lowers the likelihood of particles reaching the cathode, resulting in a decrease in particle absorption. Consequently, the weight percentage of particles incorporated into the coating decreases with increasing current density [7, 10]. A closer look at Fig. 4 reveals that the amount of deposited CeO_2 nanoparticles is higher than that of SiC. This difference can be attributed to the greater reactivity of the oxide (CeO_2) compared to SiC in bonding with the Ni matrix [2].

The microhardness values of the prepared coatings at various current densities are presented in Table 2. The results show that the hardness of the coatings decreases with increasing current density. Previous studies have indicated that at lower current densities, the coatings exhibit a larger-grained structure and reduced microhardness [10]. This can be attributed to the slow deposition rate, which allows sufficient time for the nuclei to grow, resulting in larger grain sizes and a decrease in coating hardness. As the current density increases, the discharge rate of ions at the cathode also increases. This expansion in the range of nucleation facilitates the formation of finer structures, ultimately leading to an increase in coating hardness. It is worth noting that the influence of current density on hardness is greater than that of nanoparticle concentration in the plating bath. An elevated concentration of nanoparticles in the bath causes the formation of agglomerated particles in the coating, thereby reducing its hardness. However, when a certain threshold of nanoparticle concentration in the bath is reached, an increase in current density leads to a reduction in grain size and an increase in microhardness [7, 21].

Fig. 5 illustrates the polarization curve of the Ni-Co-SiC-CeO$_2$ coating at various current densities. The corresponding results can be found in Table 2. The increase in corrosion current and the more negative corrosion potential reflect faster corrosion kinetics at higher current densities. A more negative corrosion potential indicates a greater thermodynamic tendency for corrosion at these higher current densities. The variation in the cathodic slope suggests changes in the kinetics of the cathodic reaction. The increase from 0.1 to 0.2 A/cm², followed by a decrease at 0.3 A/cm², indicates that the cathodic process may be influenced by factors such as concentration polarization or diffusion limitations. Additionally, the increase in the anodic slope suggests slower kinetics of the anodic reaction. A higher anodic slope implies that the anodic reaction rate becomes more dependent on the applied potential as the current density rises, indicating slower kinetics of the anodic reaction.
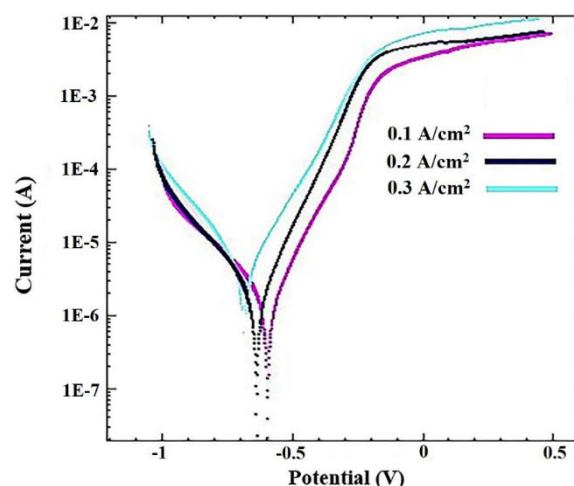
Fig. 5. Tafel curves of the coatings prepared with different current density in a 3.5% NaCl aqueous solution

At higher current densities, the cobalt content in the coating decreases while the nickel content increases. In other words, the deposition rate of nickel is relatively faster than that of cobalt with increasing current density. This is due to the fact that at higher current densities, the predominant species (Ni^{2+}) in the bath have a higher tendency to deposit kinetically compared to the less abundant species (Co^{2+}) [7,10].

Table 2. Microhardness values and results of Tafel curve fitting of the coatings prepared at a frequency of 10 Hz, duty cycle of 10% and with different current density

Current density (A/cm²)	Vickers microhardness	Corrosion current (μA/cm²)	Anodic Slop (V/decade)	Cathodic Slop (V/decade)	Corrosion voltage (mV)	Polarization resistance (Ω.cm²)
0.1	544±14	0.35	0.12	0.17	-605	872
0.2	583±16	0.45	0.13	0.22	-645	788
0.3	615±20	0.88	0.14	0.19	-685	398

Furthermore, the presence of defects and an irregular structure leads to a decrease in grain size and an increase in grain boundaries, which are more susceptible to corrosion. Consequently, the corrosion resistance decreases with increasing current density. As current density increases during electrodeposition, the thermodynamic stability of the deposited layers may be altered. Elevated current densities can lead to the formation of less stable phases or microstructures, which may exhibit greater susceptibility to corrosion [5, 10].

3.2. Investigating the Effect of Duty Cycle

To investigate the effect of duty cycle, Ni-Co-SiC-CeO$_2$ nanocomposite coatings were prepared at a current density of 0.2 A/cm^2, a frequency of 10 Hz, and duty cycles of 10, 20, and 30%. The influence of the 10% and 30% duty cycles on the surface morphology of the Ni-Co-SiC-CeO$_2$ nanocomposite coating is depicted in Fig. 6. It has been reported that as the duty cycle increases, the coatings develop rough and uneven microstructures, leading to agglomeration [15, 16]. The EDS results show that increasing the duty cycle reduces the amount of cobalt and nanoparticles in the coating (Fig. 6). Lower duty cycles result in longer off-times at a fixed pulse frequency, allowing Ni^{2+} and Co^{2+} ions to capture more nanoparticles, thereby increasing their incorporation into the coating. Conversely, higher duty cycles shorten the off-time, reducing nanoparticle concentration near the cathode, which leads to fewer nanoparticles being deposited [16, 22]. According to Guglielmi's two-step adsorption mechanism, the codeposition of inert nanoparticles involves two stages: initially, particles loosely adsorb onto the cathode with a high coverage of metal ions, and then they are transported to the cathode surface by electrophoretic attraction. They are subsequently adsorbed due to the Coulomb force between the particles and adsorbed ions [10, 23]. At a low duty cycle, the extended off-time allows more nanoparticles to reach the cathode, increasing the number of particles deposited into the coating [8, 16].
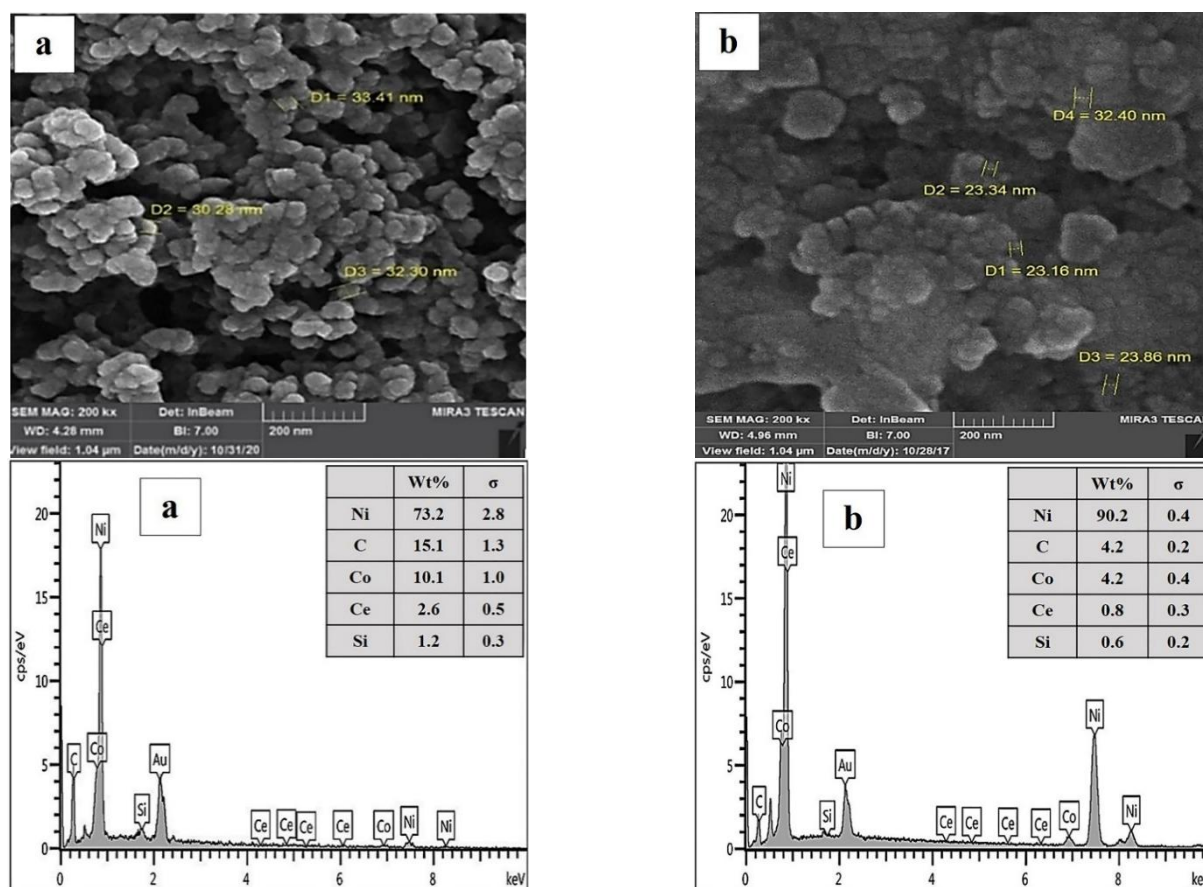

Fig. 6. SEM images and EDS results of the coatings obtained at a current density of 0.2 A/cm^2, a frequency of 10 Hz, and duty cycles: a) 10%, and b) 30%

7

The microhardness values of the prepared coatings at different duty cycles are presented in Table 4. It is observed that the hardness decreases as the duty cycle increases. This can be attributed to the reduction in the amount of SiC and CeO$_2$ in the ground phase, resulting in a decrease in their strengthening effect [8, 16]. In high duty cycles, there is a higher probability of free ions reaching the cathode surface compared to particles, leading to fewer particles being deposited in the coating. Conversely, in low duty cycles, the increased off time allows more particles to reach the cathode surface. Additionally, ions that have not been strongly absorbed are separated from the deposit surface, resulting in a dense coating with fewer defects, thus increasing the hardness in low duty cycles [5, 17]. The influence of duty cycle on the polarization curve of the Ni-Co-SiC-CeO$_2$ coating is illustrated in Fig. 7. The results of the polarization curves at different duty cycles are presented in Table 3. As the duty cycle increases, the corrosion current density also rises, indicating an accelerated rate of corrosion. This can be attributed to the decrease in off time with an increase in duty cycle, approaching the conditions of the direct current (DC) state. Due to the shorter off time, the release of hydrogen ions is reduced, resulting in higher residual stresses and more susceptible corrosion sites in the coating. Moreover, it has been reported that when the duty cycle increases significantly, the off time becomes very short. This, in turn, leads to an increase in residual stress and consequently an increase in the corrosion current [7]. The corrosion potential remains relatively constant, indicating that the overall electrochemical driving force for corrosion is not significantly affected by the duty cycle. The anodic slope is also relatively stable, while the cathodic slope shows a slight decrease. This suggests that the kinetics of the anodic reaction are less influenced by the duty cycle compared to the cathodic reaction. The data indicate that the material is in an active corrosion state under these conditions. The increasing corrosion current density and decreasing polarization resistance further confirm this. Moreover, an increase in duty cycle results in a decrease in the cobalt and nanoparticles content of the coating, leading to a decrease in corrosion resistance [7, 8, 10].
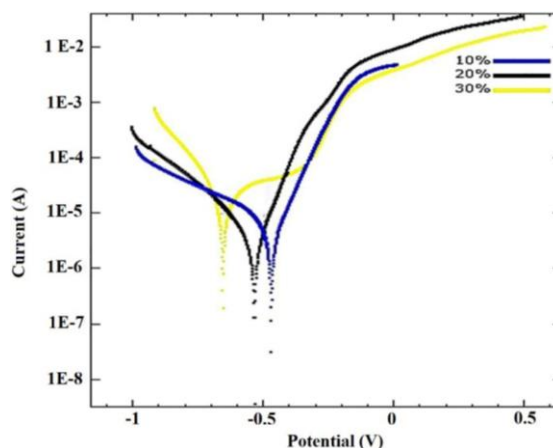
Fig. 7. Tafel curves of the coatings prepared at a current density of 0.2 A/cm^2, a frequency of 10 Hz and with different duty cycles in a 3.5% NaCl aqueous solution
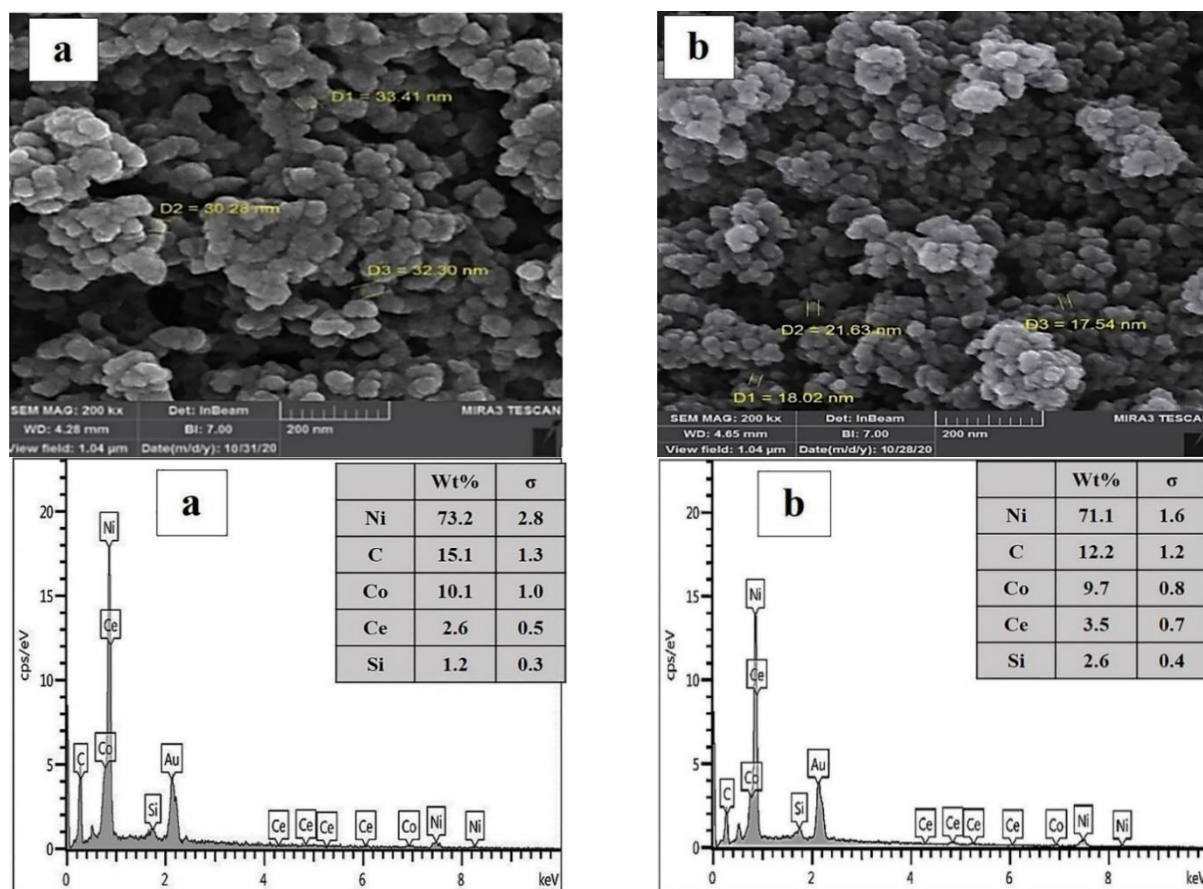
3.3. Investigating the Effect of Frequency

To investigate the impact of frequency, Ni-Co-SiC-CeO$_2$ nanocomposite coatings were prepared using a current density of 0.2 A/cm^2 and a duty cycle of 10% at frequencies of 10, 100, and 1000 Hz. The effect of frequency on the surface morphology of the nanocomposite coatings is depicted in Fig. 8. As the frequency increases, the coating becomes more uniform, smoother, and denser. The average grain size decreased from approximately 35 nm to 20 nm as the frequency increased from 10 Hz to 1000 Hz.

The results of the EDS analysis show that the content of deposited nanoparticles increases with pulse frequency. During pulse electrodeposition, higher frequencies generate greater overpotential, providing more energy for adsorbing inert particles like SiC and CeO$_2$ [8].

Table 3. Microhardness values and results of Tafel curve fitting for the coatings prepared at a current density of 0.2 A/cm^2, a frequency of 10 Hz and with different duty cycles

Duty cycle (%)	Vickers microhardness	Corrosion current (µA/cm^2)	Anodic Slop (V/decade)	Cathodic Slop (V/decade)	Corrosion voltage (mV)	Polarization resistance (Ω.cm^2)
10	583±16	0.45	0.13	0.22	-645	788
20	529±12	1.5	0.1	0.23	-584	202
30	505±15	2.14	0.1	0.13	-637	115

Fig. 8. SEM images and EDS results of the coatings prepared at a current density of 0.2 A/cm^2, duty cycle of 10% and with varying frequency: a) 10 Hz, and b) 1000 Hz

Higher pulse frequencies enhance the overpotentials of Ni^{2+} and Co^{2+} ions in the solution, providing more energy for nanoparticle adsorption. This drives more nanoparticles toward the cathode, increasing their presence in the coatings. Conversely, lower frequencies reduce the ability of metal particles to adsorb nanoparticles, resulting in fewer nanoparticles being codeposited with Ni^{2+} and Co^{2+} ions [8, 15, 16].

The impact of pulse frequency on the microhardness of Ni–Co–SiC-CeO$_2$ nanocoatings, which were deposited with a constant 10% duty cycle, is presented in Table 4. Pulse frequency plays a crucial role in determining the microhardness of these coatings. Coatings prepared with a pulse frequency of 1000 Hz exhibit the highest average microhardness of 692 Hv among all the samples. According to the literature, the microhardness of nanocoatings primarily depends on the hardness of the matrix grains and the embedded ceramic particles. Generally, the hardness of metallic matrix composites is affected by the quantity of incorporated hard particles and the hardness of the metal matrix. In the case of a specific metal matrix, the nanoparticles that are incorporated become the dominant factor influencing the microhardness of the composite. Therefore, increasing the content of ceramic nanoparticles should enhance the microhardness of coatings that employ the same matrix metal grain [8, 15, 16].

Fig. 9 shows the polarization curve of Ni-Co-SiC-CeO$_2$ coatings at various frequencies, while Table 5 provides a summary of the results. A less negative corrosion potential at higher frequencies (100 Hz and 1000 Hz) indicates a reduction in the thermodynamic driving force for corrosion, which correlates with improved resistance. The anodic slope is highest at 100 Hz (0.18 V/decade) and lower at both 10 Hz (0.13 V/decade) and 1000 Hz (0.11 V/decade). The cathodic slope varies but remains within a close range across frequencies, showing a slight increase at 10 Hz (0.22 V/decade) and 1000 Hz (0.20 V/decade). These

variations suggest changes in the reaction kinetics of the anodic and cathodic processes with frequency, possibly due to microstructural or surface property changes.
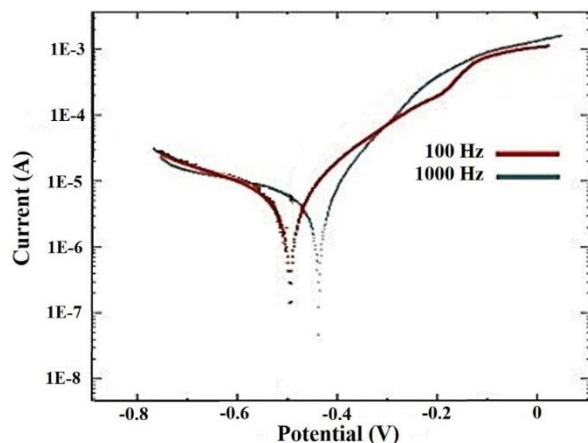
Fig. 9. Tafel curves of the coatings prepared at a current density of 0.2 A/cm^2, duty cycle of 10% and with varying frequency in a 3.5% NaCl aqueous solution

As the pulse frequency increases, the corrosion current decreases, indicating improved corrosion resistance. This improvement can be attributed to a higher incorporation of SiC and CeO$_2$ nanoparticles, which enhance the strength, hardness, structural integrity, and chemical stability of the coatings. Collectively, these factors contribute to greater corrosion resistance. Moreover, the presence of inert SiC and CeO$_2$ particles on the surface layer diminishes the effectiveness of the coating. It is also worth noting that higher frequencies reduce coating porosity, potentially leading to further enhancement in corrosion resistance [7, 8, 10, 15].

4. CONCLUSIONS

The parameters of pulse electrodeposition, including current density, duty cycle, and frequency, have a significant impact on the properties of the Ni-Co/SiC-CeO$_2$ coatings being prepared. Increasing the current density from 0.1 to 0.3 A/cm^2 led to a finer grain morphology of the coatings, as well as higher hardness and lower corrosion resistance. Additionally, the coatings prepared with a 10% duty cycle exhibited higher microhardness and corrosion resistance compared to those prepared with a 30% duty cycle. Moreover, increasing the frequency from

10 Hz to 1000 Hz resulted in higher microhardness and improved corrosion resistance of the coating.

REFERENCES

[1]. Narasimman, P, Pushpavanam, M. and Periasamy, V. M., "Synthesis, Characterization and Comparison of Sediment Electro-codeposited Nickel–Micro and Nano SiC Composites." Appl. Surf. Sci., 2011, 258, 590–598. https://doi.org/10.1016/j.apsusc.2011.08.038.

[2]. Dehgahi, S, Amini, R. and Alizadeh, M., "Microstructure and Corrosion Resistance of Ni-Al$_2$O$_3$-SiC Nanocomposite Coatings Produced by Electrodeposition Technique." J. Alloys Compd., 2016, 692, 622-628. https://doi.org/10.1016/j.jallcom.2016.08.244.

[3]. Gül, H, Kılıç, F., Uysal, M., Aslan, S., Alp, A. and Akbulut, H., "Effect of Particle Concentration on the Structure and Tribological Properties of Submicron Particle SiC Reinforced Ni Metal Matrix." Appl. Surf. Sci., 2012, 258, 4260– 4267. https://doi.org/10.1016/j.apsusc.2011.12.069.

[4]. Farhan, M, Fayyaz, O., Qamar, M. G., Shakoor, R. A., Bhadra, J. and Al-thani, N. J., "Mechanical and Corrosion Characteristics of TiC reinforced Ni-P based Nanocomposite Coatings." Mater. Today Commun., 2023, 36, 106901. https://doi.org/10.1016/j.mtcomm.2023.106901.

[5]. Roy, S, Mishra, B. M. and Bose, G. K., "Characterization of Ni-P based Poly-alloy and Composite Coatings Involving Nanoindentation and Nanoscratch Tests." Mater. Today Commun., 2021, 29, 102991. https://doi.org/10.1016/j.mtcomm.2021.102991.

[6]. Xu, Y, Fan, M., Luo, Y., Chen, Y., Hao, J. and Hou, X., "Tribology and Corrosion Properties Investigation of a Pulse Electrodeposition Duplex Hard-particle-reinforced NiMo Nanocomposite Coating." Surf. Coat. Technol., 2020, 393, 125797. https://doi.org/10.1016/j.surfcoat.2020.125797.

Table 4. Microhardness values and results of Tafel curve fitting for the coatings prepared at a current density of 0.2 A/cm², duty cycle of 10% and with different frequency

Frequency (Hz)	Vickers microhardness	Corrosion current ($\mu A/cm^2$)	Anodic Slop (V/decade)	Cathodic Slop (V/decade)	Corrosion voltage (mV)	Polarization resistance ($\Omega.cm^2$)
10	583±16	0.45	0.13	0.22	-645	788
100	625±13	0.36	0.18	0.14	-524	950
1000	692±14	0.29	0.11	0.20	-536	1063

[7]. Safavi, M. S, Tanhaei, M., Ahmadipour, M. F., Adli, R. G., Mahdavi, S. and Walsh, F. C., "Electrodeposited Ni-Co alloy-particle Composite Coatings: a Comprehensive Review." Surf. Coat. Technol., 2020, 382, 125153. https://doi.org/10.1016/j.surfcoat.2019.125153.

[8]. Yang, Y, and Cheng, Y. F., "Fabrication of Ni–Co–SiC Composite Coatings by Pulse Electrodeposition — Effects of Duty Cycle and Pulse Frequency." Surf. Coat. Technol., 2013, 216, 282–288. https://doi.org/10.1016/j.surfcoat.2012.11.059.

[9]. Shi, L, Sun, C. F., Zhou, F. and Liu, W.M., "Electrodeposited Nickel– cobalt Composite Coating Containing Nano-sized Si_3N_4." Mater. Sci. Eng. A., 2005, 397, 190–194. https://doi.org/10.1016/j.msea.2005.02.009.

[10]. Li, B. and Zhang, W., "Synthesis of Ni-Co-ZrO_2 Nanocomposites doped with Ceria Particles via Electrodeposition as Highly Protective Coating." J. Alloys Compd., 2020, 820, 153158. https://doi.org/10.1016/j.jallcom.2019.153158.

[11]. Chang, L. M., An, M. Z., Guo, H. F. and Shi, S. Y., "Microstructure and Properties of Ni–Co/nano-$A_{12}O_3$ Composite Coatings by Pulse Reversal Current Electrodeposition." Appl. Surf. Sci., 2006, 253, 2132–2137. https://doi.org/10.1016/j.apsusc.2006.04.018.

[12]. Rasooli, A, Safavi, M. S. and Hokmabad, M. K., "Cr_2O_3 nanoparticles : A Promising Candidate to Improve the Mechanical Properties and Corrosion Resistance of Ni-Co Alloy Coatings." Ceram. Int., 2018, 44, 6466-6473.

https://doi.org/10.1016/j.ceramint.2018.01.044.

[13]. Bakhit, B., "The Influence of Electrolyte Composition on the Properties of Ni-Co alloy Coatings Reinforced by SiC Nano-particles." Surf. Coat. Technol., 2015, 275, 324-331. https://doi.org/10.1016/j.surfcoat.2015.04.046.

[14]. Jiang, W, Shen, L., Wang, K., Wang, Z. and Tian, Z., "Wear Resistance of Ni-Co/SiC Composite Coating by Jet Electrodeposition in the Presence of Magnetic Field." Proc. Inst. Mech. Eng. Pt. B J. Eng. Manufact., 2020, 234, 431-438. https://doi.org/10.1177/0954405419875353.

[15]. Yu, X, Ma, Z., Li, J. and Ma, C., "Study of the Novel Ni/Co–SiC Coatings Deposited by Pulse Current Electrodeposition. Influence of the Pulse Frequency and the Duty Cycle." Int. J. Electrochem. Sci., 2021, 16, 1036. https://doi.org/10.20964/2021.03.64.

[16]. Ma, C, Zhao, D. and Ma, Z., "Effects of Duty Cycle and Pulse Frequency on Microstructures and Properties of Electrodeposited Ni–Co–SiC Nanocoatings." Ceram. Int., 2020, 46, 12128-12137. https://doi.org/10.1016/j.ceramint.2020.01.258.

[17]. You, S, Jiang, C., Wang, L., Xing, S. and Zhan, K., "Effect of CeO_2 nanoparticles on the Microstructure and Properties of the NiCo-CeO_2 Composite Coatings." Vacuum., 2022, 196, 110765. https://doi.org/10.1016/j.vacuum.2021.110765.

[18]. Srivastava, M, Grips, V. W. and Rajam, K. S., "Electrodeposition of Ni–Co Composites Containing nano-CeO_2 and their Structure, Properties." Appl.

Surf. Sci., 2010, 257, 717-722. https://doi.org/10.1016/j.apsusc.2010.07.0 46.

[19]. Fathyunes, L. and Mohtadi-Bonab, M. A., "Co-electrodeposition of Superhydrophobic NiCo/CeO$_2$ Coating with Hierarchical nano/micro Structure for Corrosion Protection of Plain Carbon Steel." Mater. Today Commun., 2024, 39, 108851. https://doi.org/10.1016/j.mtcomm.2024.10 8851.

[20]. Zhu, R, Zhu, C., Wu, S., Wan, X. and Li, G., "Effect of CeO$_2$ on Microstructure and Properties of Ni–Co-based Coatings." J. Mater. Res. Technol., 2023, 26, 7329-7339. https://doi.org/10.1016/j.jmrt.2023.09.108.

[21]. Dheeraj, P. R, Patra, A., Sengupta, S., Das, S. and Das, K., "Synergistic Effect of Peak Current Density and Nature of Surfactant on Microstructure, Mechanical and Electrochemical Properties of Pulsed Electrodeposited Ni-Co-SiC nanocomposites." J. Alloys Compd., 2017, 729, 1093-1107. https://doi.org/10.1016/j.jallcom.2017.09. 035.

[22]. Sajjadnejad, M, Setoudeh, N., Mozafari, A., Isazadeh, A. and Omidvar, H., "Alkaline Electrodeposition of Ni–ZnO Nanocomposite Coatings: Effects of Pulse Electroplating Parameters." Trans. Indian Inst. Met., 2017, 70, 1533–1541. https://doi.org/10.1007/s12666-016-0950-4.

[23]. Guglielmi, N., "Kinetics of the Deposition of Inert particles from Electrolytic Baths." J. Electrochem. Soc., 1972, 119, 1009. 10.1149/1.2404383.